Homogenization of 3D Concrete Microstructures based on CT image reconstruction

George Stefanou[1,*], Dimitrios Savvas[1] and Panagiotis Metsis[1]

[1]*Institute of Structural Analysis & Dynamics of Structures,Department of Civil Engineering, Aristotle University of Thessaloniki, 54124 Thessaloniki, Greece, *gstefanou@civil.auth.gr, dimitriosavvas@yahoo.gr, panos@metsis.gr*

Abstract. The purpose of this paper is to determine the random spatially varying elastic properties of concrete at various scales taking into account its highly heterogeneous microstructure. The reconstruction of concrete microstructure is based on computed tomography (CT) images of a cubic concrete specimen. The variability of local volume fraction of the constituents (air, cement paste and aggregates) is quantified and mesoscale random fields of the elasticity tensor are computed from a number of statistical volume elements obtained by implementing the moving window technique on the specimen along with computational homogenization. Based on the statistical characteristics of the mesoscale random fields, useful conclusions are derived regarding the effect of microstructure on the mechanical behavior of concrete.

Keywords: Concrete, CT images, Reconstruction, 3D FEM models, Homogenization, Mesoscale random fields

1. Introduction

The macroscopic mechanical properties of heterogeneous materials such as composites and concrete are significantly influenced by their underlying microstructure and can be efficiently determined using numerical homogenization techniques. The application of homogenization methods in the analysis of multi-phase materials is much more advantageous over direct simulation of the full microstructure in terms of required computational resources. The key issue in homogenization methods is the linking of micromechanical characteristics with the random variation of material properties at higher scales, which is usually established using Hill's macro-homogeneity condition (Hill, 1963). In this framework, it is necessary to identify a representative volume element (RVE) over which a fine-scale boundary value problem is solved. A possible way to achieve this is through computational convergence schemes with respect to specific apparent properties (Ostoja-Starzewski, 2006). In contrast to the RVE, which is characterized by deterministic material properties, the spatial variation of the elasticity tensor at lower scales is quantified by random fields computed on mesoscale models-statistical volume elements (SVEs) (Savvas et al., 2016a).

The scope of this paper is to determine the elastic properties of concrete at various scales taking into account the highly heterogeneous microstructure of this material which is responsible for its complex mechanical behavior. There is a wide variety of methods in the literature for the reconstruction of concrete microstructure mostly based on image processing and/or morphological random fields, e.g. (Huang et al., 2016; Huang and Peng, 2018). The reconstruction is based herein on computed tomography (CT) images of a cubic concrete specimen. The variability of local volume fraction of the constituents (air, cement paste and aggregates) is quantified first. Mesoscale random fields of the elasticity tensor are computed subsequently from a number of SVEs obtained by implementing the moving window technique on the concrete specimen along with computational homogenization. Based on the statistical characteristics of the random fields, useful conclusions are derived regarding the effect of microstructure on the mechanical behavior of concrete.

The paper is organized as follows: In Section 2, the process of reconstructing concrete microstructure based on CT images is described. Section 3 presents the framework of computational homogenization used to determine the random spatially varying apparent elasticity tensor of 3D concrete microstructures. The numerical results obtained using the proposed approach are discussed in the next section followed by some concluding remarks in Section 5.

2. Reconstruction of Concrete Microstructure based on CT Images

2.1. CT Images

Computed Tomography or "CT" has its origins in the medical field and refers to a computerized X-ray imaging procedure in which a patient is struck by a narrow X-ray beam that rotates at a certain speed around the patient's body. Although the CT procedure has been applied mainly for medical purposes, the gradual increase in available CT equipment and the improvement of the cost factors have led to other utilizations, such as the exploration of the microstructure of heterogeneous materials.

When the X-ray beam passes through a sample, some of the X-ray radiation is absorbed and scattered (with intensity I_o), while the rest penetrates through the sample (with intensity I), as shown in Figure 1.

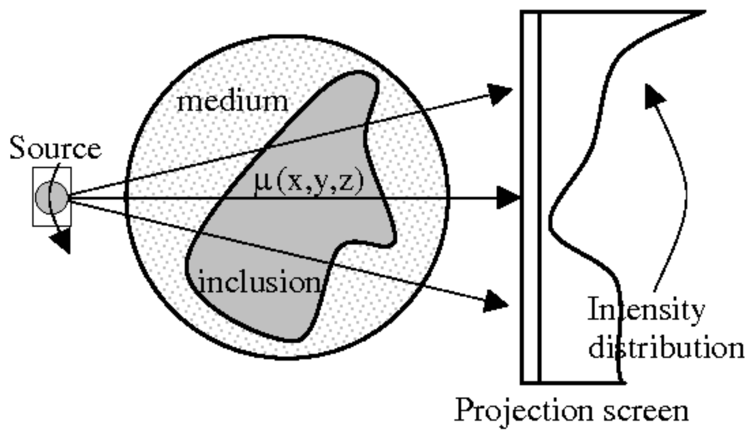

Figure 1. Intensity Distribution of an X-ray array (Daigle et al., 2005)

The radiodensity of the CT scan can be described by the Hounsfield unit (HU) scale. HU scale is a quantitative scale that reflects the linear transformation of the original linear attenuation coefficient measurement (μ) so as the radiodensity of distilled water at standard pressure and temperature is defined as zero HU, while the radiodensity of air, at the same conditions, is defined as -1000 HU. The linear transformation used to convert the attenuation values μ to Hounsfield units HU on each pixel of the CT image is as follows:

$$HU = \mu * slope + intercept \tag{1}$$

where the values of the rescale slope and intercept parameters are specific to the CT scanner system used. Their values can be obtained from the extracted DICOM (Digital Imaging and Communications in Medicine) files.

2.2. Reconstruction of concrete microstructure

The reconstruction of concrete microstructure is based on data obtained from the CT scan. The specimen is cut in 2D slices (images) with their corresponding resolution (Figure 2). Each pixel carries, beside its geometric properties, the attenuation value μ that is converted to the respective HU value using Eq. (1). Then, by utilizing voxels (the generalization of pixels on a regularly spaced, three-dimensional grid), the voxel-based FE method is employed. Using the moving window technique (Baxter et al., 2001), random mesoscale models or SVEs are created, which are discretized by a structured FE mesh based on voxels geometry. More details about the procedure of reconstruction are provided in Section 4.

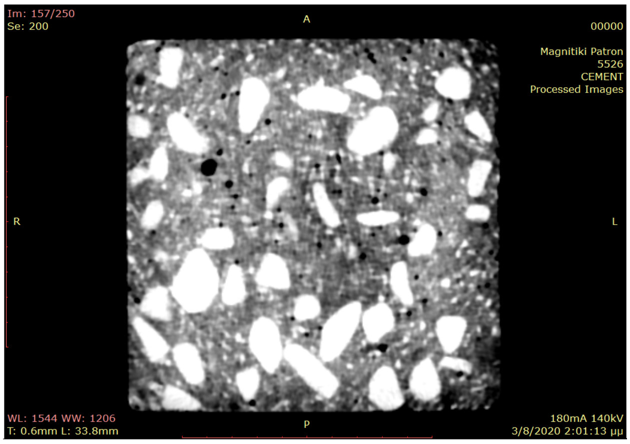

Figure 2. A 2D CT image of concrete.

3. Computational Homogenization

According to 1983, the homogenization process is based on the fundamental assumption of statistical homogeneity of the heterogeneous medium. This implies that all statistical properties of the state variables are the same at any material point and thus an RVE can be identified. While in case of composites with periodic or nearly periodic geometry the RVE is explicitly defined, in case of spatial randomness, the RVE needs to be sought using computational methods (Kanit et al., 2003; Zeman and Sejnoha, 2007; Zohdi and Wriggers, 2008; Wimmer et al., 2016; Savvas et al., 2016a; Savvas et al., 2016b).

According to 1963, the existence of the RVE postulates separation of scales in the form:

$$d \ll L \ll L_{macro} \tag{2}$$

In the above inequality, the microscale parameter d denotes a characteristic size of the fillers, e.g. their diameter in case of circular inclusions, the mesoscale parameter L denotes the size of the volume element and the macroscale parameter L_{macro} denotes the characteristic length over which the macroscopic loading varies in space, or in the case of complete scale separation, the size of the macroscopic homogeneous medium.

The statistical characteristics of the apparent elasticity tensor of concrete are computed by analyzing a set of random mesoscale models or SVEs. These are extracted by implementing the moving window technique on a cubic concrete specimen reconstructed based on a set of 2D CT images (see Section 2). Figure 3 depicts the cubic concrete specimen segmented into a large number of non-overlapping SVE models along with a detail of the voxel based FE mesh of a specific SVE. Each SVE model is characterized by the non-dimensional parameter $\delta = L/d$ with $\delta \in [1, \infty]$, which denotes the scale factor. Note that the length scale of the SVE is smaller than the one of the corresponding RVE. For each placement of the moving window, the apparent material properties are computed through homogenization of the material in the microscale. The resulting mesoscale properties and corresponding moving window centres are used to build the related random field model, as shown in Section 4.

3.1. Computation of the Random Apparent Elasticity Tensor of 3D Concrete Microstructures

The stress and strain fields, $\boldsymbol{\sigma}(\omega, \boldsymbol{x})$ and $\boldsymbol{\varepsilon}(\omega, \boldsymbol{x})$ respectively, developed on the mesoscale realization of concrete $B_\delta(\omega)$ can be expressed as a superposition of means ($\bar{\boldsymbol{\sigma}}$ and $\bar{\boldsymbol{\varepsilon}}$) and of zero-mean fluctuations ($\boldsymbol{\sigma}'$ and $\boldsymbol{\varepsilon}'$) as follows:

$$\boldsymbol{\sigma}(\omega, \boldsymbol{x}) = \bar{\boldsymbol{\sigma}} + \boldsymbol{\sigma}'(\omega, \boldsymbol{x}) \quad , \quad \boldsymbol{\varepsilon}(\omega, \boldsymbol{x}) = \bar{\boldsymbol{\varepsilon}} + \boldsymbol{\varepsilon}'(\omega, \boldsymbol{x}) \tag{3}$$

The means of stress and strain tensors at some point $\boldsymbol{X}$ of the macro-continuum are computed as volume averages over $B_\delta(\omega)$ in the form (Hill, 1963):

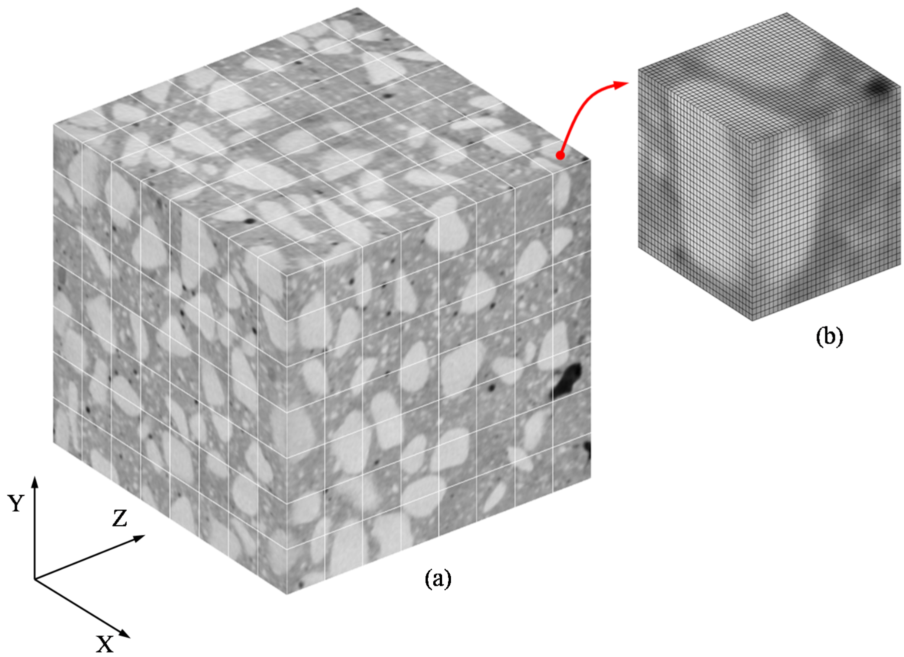

Figure 3. a) Schematic of 3D moving window technique on a cubic concrete specimen reconstructed using 2D CT images, b) Detail of the voxel based FE mesh of a specific SVE model.

$$\bar{\boldsymbol{\sigma}}(\omega, \boldsymbol{X}) = \frac{1}{V_\delta} \int\limits_{B_\delta(\omega)} \boldsymbol{\sigma}\left(\omega, \boldsymbol{x}\right) \mathrm{d}V_\delta, \;\; \bar{\boldsymbol{\varepsilon}}(\omega, \boldsymbol{X}) = \frac{1}{V_\delta} \int\limits_{B_\delta(\omega)} \boldsymbol{\varepsilon}\left(\omega, \boldsymbol{x}\right) \mathrm{d}V_\delta \tag{4}$$

with $V_\delta = \int\limits_{B_\delta(\omega)} \mathrm{d}V_\delta$.

Also the volume average of the strain energy can be calculated as:

$$\bar{U} = \frac{1}{2V_\delta} \int\limits_{B_\delta(\omega)} \boldsymbol{\sigma}\left(\omega, \boldsymbol{x}\right) : \boldsymbol{\varepsilon}\left(\omega, \boldsymbol{x}\right) \mathrm{d}V_\delta = \frac{1}{2}\overline{\boldsymbol{\sigma} : \boldsymbol{\varepsilon}} = \frac{1}{2}\bar{\boldsymbol{\sigma}} : \bar{\boldsymbol{\varepsilon}} + \frac{1}{2}\overline{\boldsymbol{\sigma'} : \boldsymbol{\varepsilon'}} \tag{5}$$

Note that for an unbounded space domain ($\delta \to \infty$) the fluctuation terms in Eq. (5) become negligible $\left(\overline{\boldsymbol{\sigma'} : \boldsymbol{\varepsilon'}} = 0\right)$ and thus the following equation holds:

$$\overline{\boldsymbol{\sigma} : \boldsymbol{\varepsilon}} = \bar{\boldsymbol{\sigma}} : \bar{\boldsymbol{\varepsilon}} \tag{6}$$

which is known as Hill's condition. However, at a finite mesoscale size, Hill's condition is valid provided that the following constraint is satisfied (Hazanov and Huet, 1994):

$$\int_{\partial B_\delta} (t - \bar{\boldsymbol{\sigma}} \cdot n) \cdot (u - \bar{\boldsymbol{\varepsilon}} \cdot \boldsymbol{x}) \, \mathrm{d}S = 0 \tag{7}$$

The constraint equation (7) is a priori satisfied by appropriate boundary conditions such as uniform strains (Dirichlet), uniform stresses (Neumann), uniform orthogonal-mixed boundary conditions and periodic boundary conditions. Here, we focus on the case of uniform strains. We now discuss the computational homogenization procedure for this case, following 2002.

In general the 3D elasticity tensor $\bar{\mathbb{C}}$, which is of 4^{th} order, consists of $3^4 = 81$ components. These are reduced to 21 independent components due to symmetries in stress and strain tensors. Thus, the macroscopic linear constitutive relation for an anisotropic material is as follows:

$$\bar{\boldsymbol{\sigma}} = \bar{\mathbb{C}}\bar{\boldsymbol{\varepsilon}} \Rightarrow \begin{bmatrix} \bar{\sigma}_{11} \\ \bar{\sigma}_{22} \\ \bar{\sigma}_{33} \\ \bar{\sigma}_{12} \\ \bar{\sigma}_{23} \\ \bar{\sigma}_{31} \end{bmatrix} = \begin{bmatrix} \bar{C}_{1111} & & & & & \text{sym} \\ \bar{C}_{2211} & \bar{C}_{2222} & & & & \\ \bar{C}_{3311} & \bar{C}_{3322} & \bar{C}_{3333} & & & \\ \bar{C}_{1211} & \bar{C}_{1222} & \bar{C}_{1233} & \bar{C}_{1212} & & \\ \bar{C}_{2311} & \bar{C}_{2322} & \bar{C}_{2333} & \bar{C}_{2312} & \bar{C}_{2323} & \\ \bar{C}_{3111} & \bar{C}_{3122} & \bar{C}_{3133} & \bar{C}_{3112} & \bar{C}_{3123} & \bar{C}_{3131} \end{bmatrix} \begin{bmatrix} \bar{\varepsilon}_{11} \\ \bar{\varepsilon}_{22} \\ \bar{\varepsilon}_{33} \\ \bar{\varepsilon}_{12} \\ \bar{\varepsilon}_{23} \\ \bar{\varepsilon}_{31} \end{bmatrix} \tag{8}$$

The unknown macroscopic elasticity components $\bar{C}_{ijkl}$, with $i, j, k, l = 1, 2, 3$, are equal to the macroscopic stresses $\bar{\sigma}_{ij}$ which are derived by the solution of six independent kinematic uniform boundary value problems (BVPs). In each BVP the displacement boundary conditions are obtained by a prescribed uniform strain tensor as shown below:

$$\bar{\boldsymbol{\varepsilon}} = \left\{ \begin{bmatrix} \bar{\varepsilon}_{11} \\ 0 \\ 0 \\ 0 \\ 0 \\ 0 \end{bmatrix}, \begin{bmatrix} 0 \\ \bar{\varepsilon}_{22} \\ 0 \\ 0 \\ 0 \\ 0 \end{bmatrix}, \begin{bmatrix} 0 \\ 0 \\ \bar{\varepsilon}_{33} \\ 0 \\ 0 \\ 0 \end{bmatrix}, \begin{bmatrix} 0 \\ 0 \\ 0 \\ \bar{\varepsilon}_{12} \\ 0 \\ 0 \end{bmatrix}, \begin{bmatrix} 0 \\ 0 \\ 0 \\ 0 \\ \bar{\varepsilon}_{23} \\ 0 \end{bmatrix}, \begin{bmatrix} 0 \\ 0 \\ 0 \\ 0 \\ 0 \\ \bar{\varepsilon}_{31} \end{bmatrix} \right\} \tag{9}$$

The imposed displacements on the boundary nodes of each SVE are calculated through the prescribed uniform strain tensor using the following equation:

$$\boldsymbol{u}_b = D_b^T \bar{\boldsymbol{\varepsilon}} \tag{10}$$

where D_b is a geometric matrix which depends on the coordinates of the boundary node b and is defined as:

$$D_b = \frac{1}{2}\begin{bmatrix} 2x & 0 & 0 \\ 0 & 2y & 0 \\ 0 & 0 & 2z \\ y & x & 0 \\ 0 & z & y \\ z & 0 & x \end{bmatrix} \quad \text{with} \quad (x, y, z) \in \boldsymbol{x} \tag{11}$$

The BVP which has to be solved is as follows:

$$\begin{bmatrix} \boldsymbol{K}_{ii} & \boldsymbol{K}_{ib} \\ \boldsymbol{K}_{bi} & \boldsymbol{K}_{bb} \end{bmatrix} \begin{bmatrix} \boldsymbol{u}_i \\ \boldsymbol{u}_b \end{bmatrix} = \begin{bmatrix} \boldsymbol{f}_i \\ \boldsymbol{f}_b \end{bmatrix} \tag{12}$$

where the stiffness matrix $\boldsymbol{K}$ of the FE model is rearranged into four sub-matrices associated with interior nodes i and boundary nodes b. The macroscopic stress tensor is then calculated as a volume average by:

$$\bar{\boldsymbol{\sigma}} = \frac{1}{V}\mathbb{D}\boldsymbol{f}_b \tag{13}$$

where $\boldsymbol{f}_b = \boldsymbol{K}_{bb}\boldsymbol{u}_b + \boldsymbol{K}_{bi}\boldsymbol{u}_i$ is the vector containing the computed reaction forces on the boundary nodes, $\boldsymbol{u}_i = \boldsymbol{K}_{ii}^{-1}\left(\boldsymbol{f}_i - \boldsymbol{K}_{ib}\boldsymbol{u}_b\right)$ is the vector containing the calculated displacements of the interior nodes and $\mathbb{D} = [D_1\ D_2\ ...\ D_M]$ with M the total number of boundary nodes b.

4. Numerical Results and Discussion

In this section, numerical results concerning the determination of the random fields of the homogenized elasticity tensor of the 3D concrete specimen are presented. The reconstruction of the microstructure of concrete is based on DICOM data obtained by a medical CT scan conducted at Magnitiki Patron S.A. The equipment used was a LightSpeed VCT of GE Medical Systems with peak potential and current applied to the X-ray tube equal to 140 kV and 180 mA, respectively. The axial resolution of the scan was fixed at 0.625 mm resulting in 211 total slices, while the pixel resolution of the 2D image in each slice plane is $0.4883 \times 0.4883\ mm^2$, resulting in $281{\times}281$ pixels. Note that the dimensions of the scanned cubic concrete specimen was approximately $136.724 \times 136.724 \times 131.25\ mm^3$.

As shown in Figure 3, the size of each SVE corresponds to that of the selected 3D window in the moving window technique. In the context of FE simulation, the discretization of the SVEs into hexahedral solid elements is based on the voxels which are used to reconstruct the 3D geometry of the concrete specimen. Information about the pixels (e.g. location, spacing, attenuation values μ) and the slices (e.g. position, thickness) needed in order to construct the voxels and also to identify the constituent materials is included in the DICOM files provided by the CT scan system. In the FE mesh of the SVEs each hexahedral solid element corresponds to a voxel. The nodes of each element correspond to pixels which are lying in two subsequent slice planes. The material assigned to each integration point of an element depends on the HU value of the integration point which is calculated by interpolating the nodal HU values using the shape functions of the element.

Figure 4 depicts the histogram (empirical distribution) of the Hounsfield units (HU) calculated by Eq. (1) with rescale slope and rescale intercept equal to 1 and -1024, respectively, for the CT equipment used. From this figure, the constituent materials (air, cement and aggregates) can be distinguished by defining specific ranges for their HU values. Based on the observed peaks of the histogram and after careful inspection of the CT images, the HU range can be selected as [-960, 800] for air, [800, 2000] for cement and [2000, 2974] for aggregates. Figure 4 depicts also a gray scale colorbar connected to the HU values of the constituent materials of concrete. The illustration of concrete specimen in Figure 3 is based on this color range.

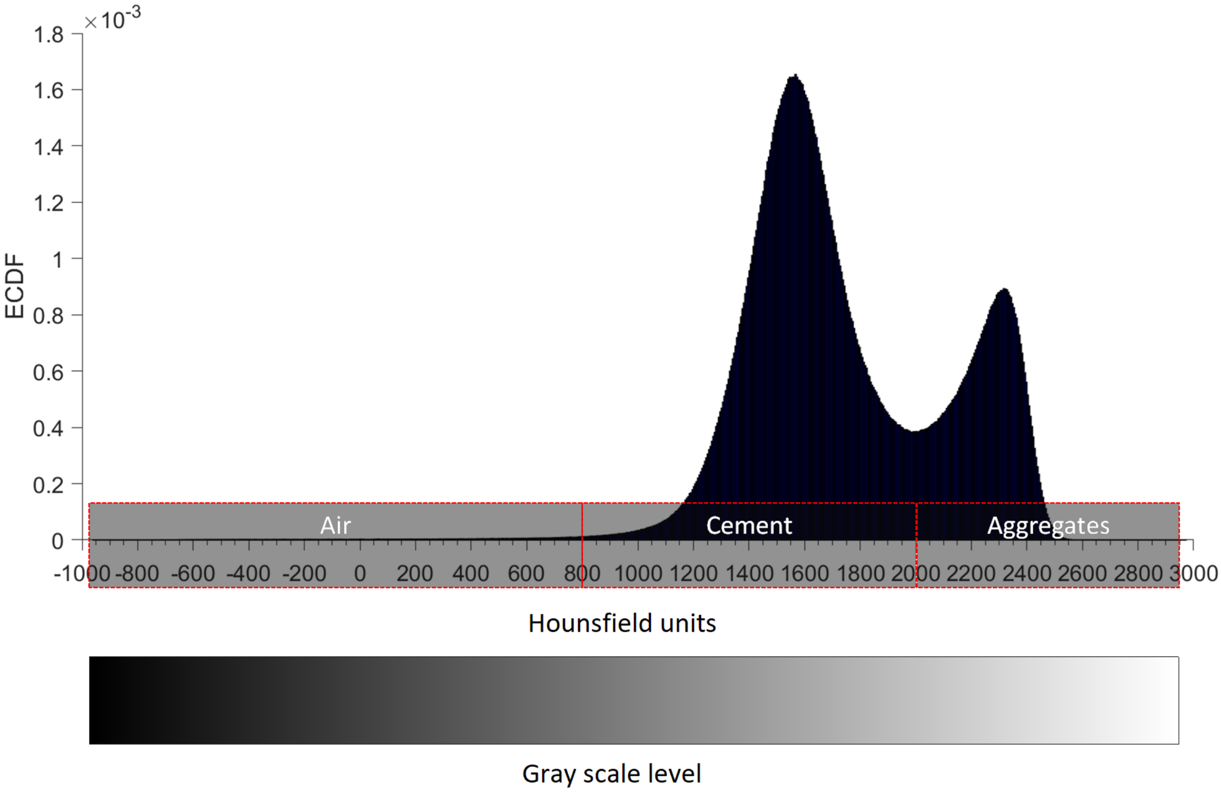

Figure 4. Empirical distribution of HU values derived from all CT images followed by the range of HU for concrete constituent materials.

Based on the aforementioned HU ranges, the local volume fraction (vf) variability of the constituents of concrete can be studied next. Figure 5 illustrates the computed 3D random fields along with the respective empirical distributions of the volume fraction of the constituent materials. For visualization purposes, Figures 5, 6 and 8 provide 2D contour plots of the random fields corresponding to the three orthogonal planes (XY, YZ and ZX) intersected at the center point of the cubic concrete specimen. Note that, these results have been obtained by selecting the size of the moving window to be $10 \times 10 \times 10$ voxels and the moving step to be equal to that size in each direction so as non-overlapping SVEs to be extracted. For this specific choice of window size and due to the dimensions of the cubic concrete specimen, the total number of the extracted SVEs is 16464. The dispersion of aggregates within cement is not uniform. Also, some air was trapped inside the paste during the mixture process. These facts are obvious in Figure 5, where regions of material rich or poor in aggregates and air can be observed. The mean vf of the constituents in the concrete specimen is 0.5% air, 72.3% cement and 27.2% aggregates.

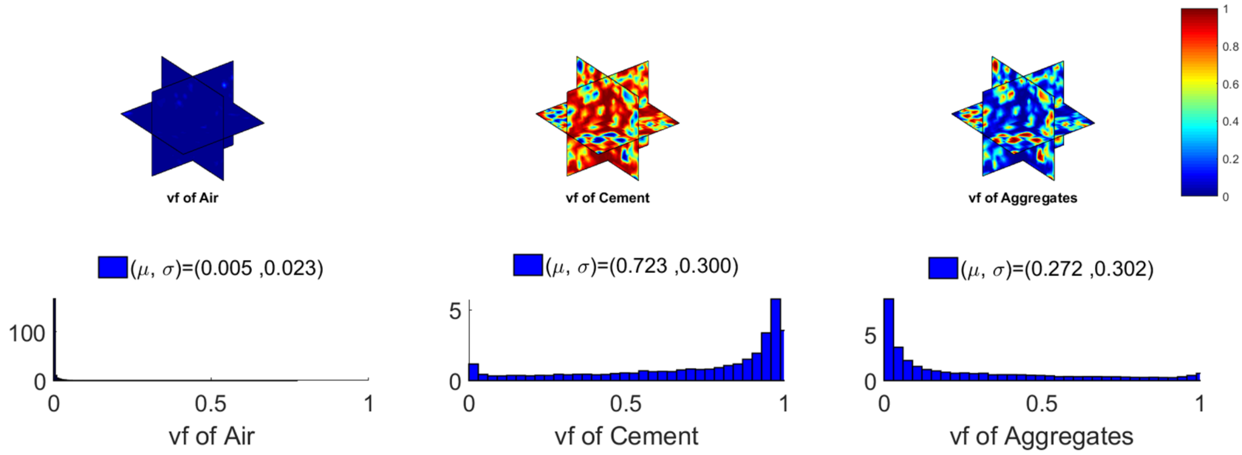

Figure 5. Random fields and histograms of vf of air, cement and aggregates.

Figures 6-9 depict the computed random fields along with the respective empirical distributions of the components of the apparent elasticity tensor (see Eq. (8)). These results have been obtained by implementing the homogenization method presented in Section 3. The constituent materials of concrete are considered linear elastic. Specifically, their Young's modulus and Poisson ratio [E, v] are assumed as [20 GPa, 0.2] for cement and [100 GPa, 0.2] for aggregates. Note that although air is not an elastic material, it can be modeled by setting its Young's modulus equal to 0.2 GPa (1% of the Young's modulus of cement) and its Poisson ratio equal to 0.45 (almost incompressible material). From the calculated mean values of the elasticity components it can be deduced that concrete can be considered as isotropic material in an average sense (Figures 7 and 9). Another observation is that the coefficient of variation (COV) of the axial and shear components of the apparent elasticity tensor is higher than 60%, which means that morphological uncertainty leads to significant random spatial variation of the mechanical properties of concrete.

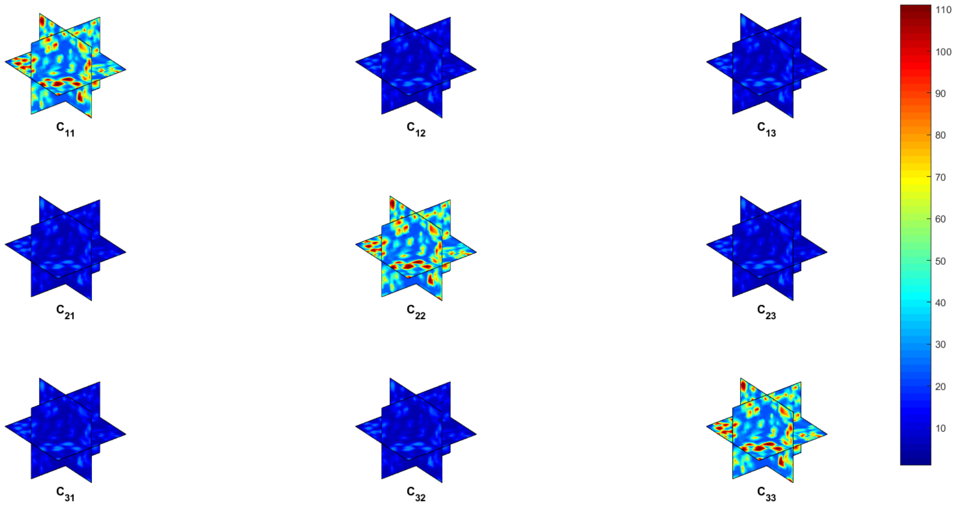

Figure 6. Random fields of $\bar{C}_{iijj}$ (correspondence of subscripts: $1 \rightarrow 11$, $2 \rightarrow 22$, $3 \rightarrow 33$).

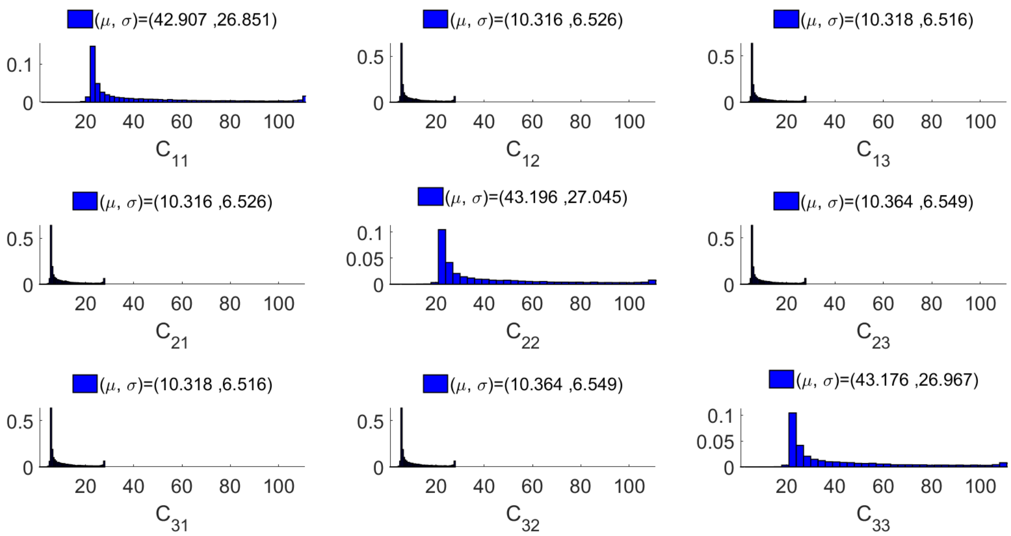

Figure 7. Histograms of $\bar{C}_{iijj}$ (correspondence of subscripts: $1 \rightarrow 11$, $2 \rightarrow 22$, $3 \rightarrow 33$).

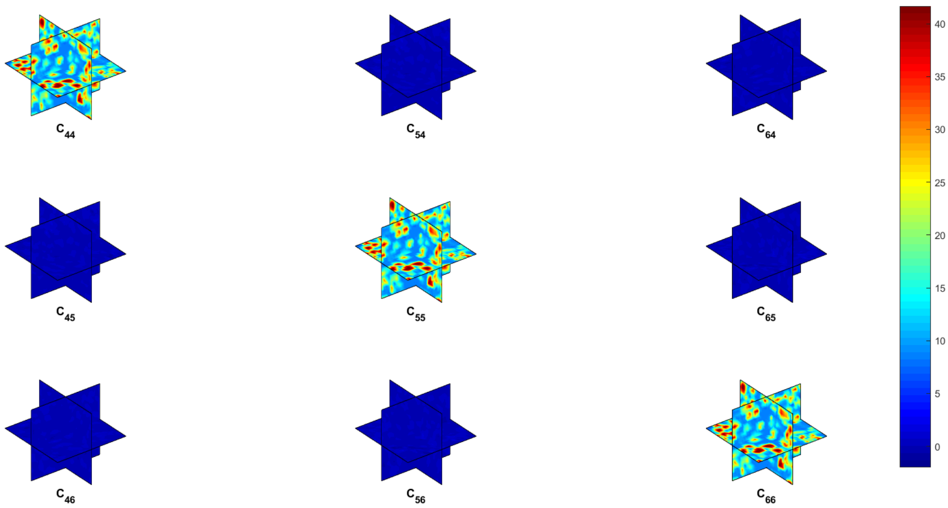

Figure 8. Random fields of $\bar{C}_{ijij}$ (correspondence of subscripts: $4 \to 12$, $5 \to 23$, $6 \to 31$).

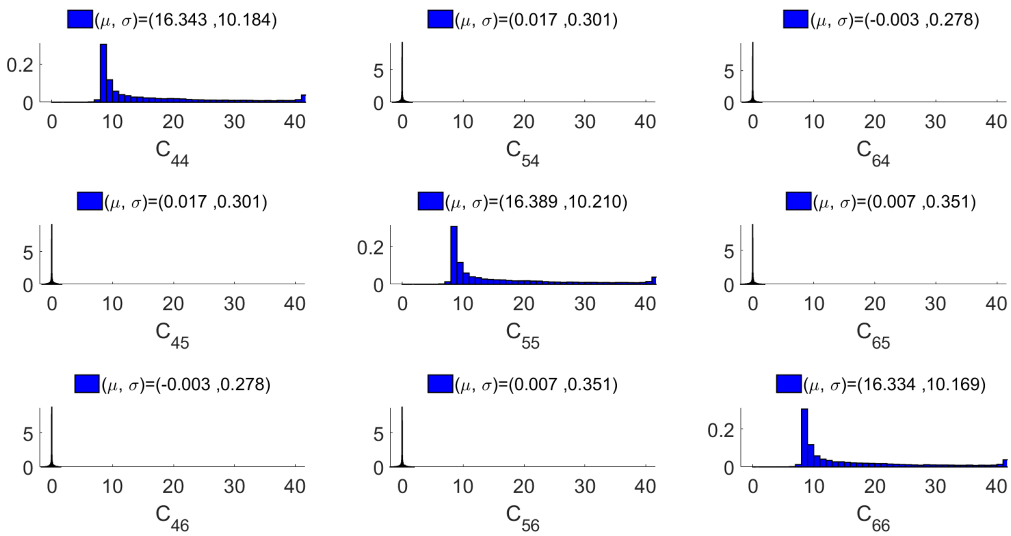

Figure 9. Histograms of $\bar{C}_{ijij}$ (correspondence of subscripts: $4 \to 12$, $5 \to 23$, $6 \to 31$).

5. Conclusions

In this paper, the random spatially varying apparent elasticity tensor of 3D concrete microstructures has been computed using CT images of a cubic specimen for the reconstruction of concrete microstructure and computational homogenization. A large variability of the local volume fraction of the constituents (air, cement paste and aggregates) has been observed. This was reflected on the high COV (>60%) of the axial and shear components of the apparent elasticity tensor, meaning that microstructural uncertainty leads to substantial random spatial variation of the mechanical properties of concrete, which has to be taken into account for a safe design of concrete structures.

Acknowledgements

This research is co-financed by Greece and the European Union (European Social Fund-ESF) through the Operational Programme "Human Resources Development, Education and Lifelong Learning 2014-2020" in the context of the project "Stochastic multiscale modeling of concrete structures reinforced with graphene nanoparticles - Investigation of the effect of nano-inclusions on the mechanical properties of concrete" (MIS 5047867). The authors wish also to acknowledge Magnitiki Patron S.A. (https://www.magnitikipatron.com/) for conducting the CT scans on the concrete specimen and providing all the necessary DICOM files in order to accomplish the present research work.

European Union
European Social Fund

Operational Programme
Human Resources Development,
Education and Lifelong Learning
Co-financed by Greece and the European Union

ΕΣΠΑ
2014-2020
ανάπτυξη - εργασία - αλληλεγγύη

References

Hill, R. Elastic properties of reinforced solids: some theoretical principles. *Journal of the Mechanics and Physics of Solids*, 11(5):357–372, 1963.

Ostoja-Starzewski, M. Material spatial randomness: From statistical to representative volume element. *Probabilistic engineering mechanics*, 21(2):112–132, 2006.

Savvas, D., G. Stefanou, and M. Papadrakakis. Determination of RVE size for random composites with local volume fraction variation. *Computer Methods in Applied Mechanics and Engineering*, 305:340–358, 2016a.

Huang, Y., D. Yan, Z. Yang, and G. Liu. 2D and 3D homogenization and fracture analysis of concrete based on in-situ X-ray Computed Tomography images and Monte Carlo simulations. *Engineering Fracture Mechanics*, 163:37–54, 2016.

Huang, J. and Q. Peng. A fast algorithm for multifield representation and multiscale simulation of high-quality 3D stochastic aggregate microstructures by concurrent coupling of stationary Gaussian and fractional Brownian random fields. *International Journal for Numerical Methods in Engineering*, 115(3):328–357, 2018.

Daigle, M., D. Fratta, and LB. Wang. Ultrasonic and X-ray tomographic imaging of highly contrasting inclusions in concrete specimens. *Site Characterization and Modeling*, 1–12, 2005.

Baxter, SC., M. Imran Hossain, and L. Graham. Micromechanics based random material property fields for particulate reinforced composites. *International journal of solids and structures*, 38:9209–9220, 2001.

Hashin, Z. Analysis of composite materials: A survey. *Journal of Applied Mechanics*, 50(2):481–505, 1983.

Kanit, T., S. Forest, I. Galliet, V. Mounoury and D. Jeulin. Determination of the size of the representative volume element for random composites: statistical and numerical approach. *International journal of solids and structures*, 40(13):3647–3679, 2003.

Zeman, J., and M. Sejnoha. From random microstructures to representative volume elements. *Modelling and Simulation in Materials Science and Engineering*, 15(4):325–335, 2007.

Zohdi, T. I., and P. Wriggers. An Introduction to Computational Micromechanics, 2nd Edition, Lecture Notes in Applied and Computational Mechanics. *Springer, Heidelberg*, 20, 2008.

Wimmer, J., B. Stier, J.-W. Simon, and S. Reese. Computational homogenisation from a 3D finite element model of asphalt concrete–linear elastic computations. *Finite Elements in Analysis and Design*, 110:43–57, 2016.

Savvas, D., G. Stefanou, V. Papadopoulos, and M. Papadrakakis. Effect of waviness and orientation of carbon nanotubes on random apparent material properties and RVE size of CNT reinforced composites. *Composite Structures*, 152:870–882, 2016b.

Hazanov, S., and C. Huet. Order relationships for boundary conditions effect in heterogeneous bodies smaller than the representative volume. *Journal of the Mechanics and Physics of Solids*, 42(12):1995–2011, 1994.

Miehe, C., and A. Koch. Computational micro-to-macro transitions of discretized microstructures undergoing small strains. *Archive of Applied Mechanics*, 72(4-5):300–317, 2002.